Journal of Experimental Microbiology and Immunology (JEMI) Vol. 17: 104 – 108


# Investigation of the pBR322 Exclusion Effect using Putative Rop Mutant pBR322 Plasmid pCAWK

**Tammy Kang**
*Department of Department & Immunology, University of British Columbia*

**Rop, repressor of primer, protein has been implicated in causing or contributing to plasmid pBR322 exclusion from *Escherichia coli* host cells. A recent study successfully created pCAWK, a putative mutated pBR322 plasmid with a non-functioning Rop protein. Whole cell PCR was performed with DH5α *E. coli* colonies respectively containing pUC19, pBR322, pCAWK1, and pCAWK2 (plasmids with different orientations of the 34 bp insert disrupting the *rop* gene) to compare plasmid copy numbers. Unique forward and reverse primers were designed through manual selection of sequences for each plasmid, complemented and optimized by analyses using primer3, REPFIND, and EMBOSS programs. Following PCR, the plasmid copy numbers of each plasmid were assessed by visual and quantitative agarose gel analysis to observe whether pCAWK in either orientation exists at a quantity that is higher, lower, or comparable to the other plasmids. Both pCAWK1 and pCAWK2 persisted poorly in host cells when compared to the parental pBR322 or pUC19, with pUC19 being most abundant. Although superficially these observations suggest that Rop may not be an important factor in the exclusion effect, the semi-quantitative technique used makes definitive conclusions difficult. The results may instead, however, reveal a problem with pCAWK being a viable tool in studying the exclusion effect and that more quantitative investigations should be conducted to conclusively determine pCAWK's utility before applying it in future Rop studies.**

ColE1-type plasmids are commonly used in experimental molecular biology (2). Although pUC19 and pBR322 belong to this family, upon co-transformation into *E. coli*, pBR322 disappears from the cell while pUC19 persists. The cause of this exclusion effect has been attributed to various possibilities, including pBR322's larger size, the presence of *rop* gene, and the lack of a point mutation which exists in pUC19 (2, 11). Compared to the 2686 bp-length of pUC19, pBR322 is 4361 bp, which means each replication cycle is less efficient. The pBR322 vector also contains a gene which encodes for Rop, or repressor of primer, protein that has been implicated in depressing gene copy number of plasmids (2). Finally, pBR322 is lacking a G to A mutation in RNAII that is conversely present in pUC19. In plasmids with ColE1 origin such as pUC19 and pBR322, RNAII forms the primer for initiation of DNA synthesis while RNAI and Rop protein have contrarily negative regulatory functions. RNAI binds to RNAII to stop primer formation and Rop stabilizes this complex (2, 11). The point mutation in pUC19 is responsible for destabilizing the formation of the RNA I—RNA II structure, enhancing replication initiation for pUC19 (11). Various approaches were attempted to isolate the effect of the Rop protein, including PCR site-directed mutagenesis, to little or no avail (5). A recent project by Airo *et al.* focused on the role of Rop protein in pBR322 exclusion by creating a construct named pCAWK (1). This plasmid is 4395 bp in size, and is sequentially identical to pBR322 with the exception of a 34 bp insert disrupting the *rop* gene (1). The 34 bp insert features stop codons in either direction, regardless of the two possible orientations depending on the direction that the insert becomes ligated into the pBR322 sequence, creating a post-translational *rop* gene mutant (1). Assuming that this pBR322 variant does not produce a functioning Rop, the following study attempted to use pCAWK to isolate the role of this protein in the pBR322 exclusion effect.

## MATERIALS AND METHODS

**Media Preparation.** 10X Tris-Borate EDTA stock was made with 108 g of Tris base (108 g Tris Base (Lot#1382726, Cat#15504-020; Invitrogen), 55 g boric acid (Lot#43024326, Cat# BX0865-1; EM Science, VWR CANLAB), 7 g EDTA (Lot#1382726, Cat# EX0539-1; EMD Bioscience, VWR CANLAB) and was subsequently diluted to 1X for further use in agarose gel making and running electrophoresis reactions. LB agar plates were formulated with (1.5 % (w/v) agar (Invitrogen, Cat. #30391-023)). These were poured to 10 mL thickness into petri plates and stored at 4 °C until use.

***E.coli* strains and plasmids.** DH5α respectively containing plasmids pUC19, pBR322, and pCAWK1 and pCAWK2 were obtained from the MICB 421 culture collection at the University of British Columbia, which were isolated in a study by Airo *et al* (1). The frozen stocks were taken from -80 °C, thawed, and subsequently plated onto LB agar.

**Primer Design.** Primers for pUC19 were generated by an online software primer3, which was used by Lee *et al*. in RT-qPCR quantification of plasmid copy numbers (6, 9). To ensure that pBR322 is uniquely identified, the forward primer was derived from 20 base pairs within the *rop* gene sequence. The pBR322 plasmid and forward primer sequences were submitted into primer3 program which in turn generated the complementing reverse primer sequence. Primer sequences for pCAWK also had to be designed manually since the only region of distinction from pBR322 was the 34 bp insert. Two distinct sets of primers were needed for pCAWK1 and pCAWK 2 since the insert into the pBR322 sequence could occur in two orientations (pCAWK1: A-B orientation, and pCAWK2: B-A orientation). The two forward primers for pCAWK1 and 2 were manually located by looking at the pBR322 sequence with the 34 bp insert oriented in both

possible directions and finding 20 consecutive base pairs containing a fair balance of the insert as well as portions of the surrounding sequence. Reverse primers for pCAWK were determined with primer3. The final step in primer design was scanning all sequences for potential secondary structure formation through REPFIND and EMBOSS explorer (4). Table 1 displays the finalized primer sequences as submitted to Integrated DNA Technologies (IDT). After receipt of primers from IDT, these were centrifuged to sediment the DNA to the bottom of the tubes prior to the opening and addition of sterile distilled water. All primers were made up to 100 µM stock and stored at -20 °C.

**TABLE 1** Projected primer sets generated by manual efforts coupled with Primer3, REPFIND, and EMBOSS.

| Plasmid | Primer Sequence | Tm (°C) | gc% | Size (bp) |
|---|---|---|---|---|
| pCAWK 1: A – B | F:gctttaccgcctggatcgat | 63 | 55 | 247 |
| | B:tgccgcatagttaagccagt | 60 | 50 | |
| pCAWK 2: B – A | F:ctagctaggtcagctgcctc | 57 | 60 | 249 |
| | B:cgcatatggtgcactctcag | 60 | 55 | |
| pBR322 | F: ctttaccgcagctgcctcgc | 67 | 65 | 247 |
| | B:cgcatatggtgcactctcag | 60 | 66 | |
| pUC19 | F:cggcatcagagcagattgta | 59 | 50 | 158 |
| | B:ctggcgtaatagcgaagagg | 60 | 55 | |

**Preparation for Whole Cell PCR.** Well-separated and morphologically round *E. coli* DH5α colonies respectively carrying plasmids pUC19; pBR322; and pCAWK 1 and 2 were sampled with sterile pipet tips and transferred to 20 µl of autoclaved $dH_20$. These were heat-treated at 94 °C using a PCR machine for 10 minutes, and were subsequently incubated for a minimum of 10 minutes at -80 °C. The tubes were finally centrifuged at 13000 rpm for 10 minutes in an eppendorf microfuge to generate supernatants and lysed cell pellets. The supernatant was used as the template DNA.

**Whole Cell PCR conditions.** Each 25 ul PCR reaction consisted of the components seen in Table 2. The Biometra® T Gradient (Software version 4.15) PCR machine was set to denature for 4 min at 94 °C prior to 35 cycles of amplification under the following conditions: denaturing at 94 °C for 45 sec, annealing at 56 °C for 30 sec and then elongation at 72 °C for 90 sec. The final step was a 10 min extension at 72 °C, end-capped by a 4 °C pause (7, 8, 10).

**Gel Electrophoresis.** All PCR reactions were simultaneously resolved on one 1.5 % (w/v) agarose gel composed of Invitrogen agarose (Lot #1137923 Cat#15510027), and run with premade 1X TBE. Each 25 ul PCR reaction was mixed with 5 ul of 6X DNA loading buffer, and 17 ul of this mixture was loaded per lane. 10 ul of the GeneRuler™ 100 bp ladder Plus (0.25 – 2.5 µg/well; Lot#00028313 Cat# SM0321; Fermentas) was included for sizing purposes. The gels were subsequently run for 1 hr at 75 V, room temperature. Post run, the gels were stained in 0.5ug/mL ethidium bromide bath overnight.

**Band analysis.** The AlphaImager tool SpotDensor was used to quantify the DNA in each band based on pixel count. Each fragment of interest was isolated by manually drawing individual boxes around its perimeter (not shown) according to the recommendations in the AlphaImager manual (3). The machine measured the degree of saturation of DNA as they appeared within the boxes, accounting for background, and outputting the data as integrated pixel density values.

## RESULTS

In Figure 1, the bands of interest are within the rectangular area, and were identified according to predicted sizes 158 for pUC19, 247 for pBR322 and pCAWK1, as well as 249 bp for pCAWK2. The molecular weight standard in lane 8 concurs with the size estimates; pBR322 as well as pCAWK1 and pCAWK2 have run similar distances (between 500 and 200) while pUC19 moved past the 200 mark, which again corresponds to expectations. Lane 7 contains the negative DNA control; the visible band in this lane is likely an accumulation of dNTP's and primers. Visually, lanes 5 (pBR322) and 6 (pUC19) seem to feature the brightest bands. Table 3 contains machine-observed data that confirm this manual observation. The Integrated Density Values (IDVs) and % columns in the table explain the following: IDV is the sum of all pixel values of each band after background correction while the % represents the percentage of the band density proportional to the total density measured on the gel. Figure 2 and Table 4 are digested forms of the numerical and visual data seen in Figure 1 and Table 3. Figure 2 accounts for the variability in PCR product sizes and how this impacts visualization of the DNA bands; the importance of taking this factor into account is explained in the Discussion section. Even after this calibration, the pUC19 PCR product and hence plasmid copy number appears highest (leftmost and highest bar in Figure 2), though the replicate pUC19R (farthest right in Figure 2) is lower and seems more comparable to pBR322 and even pCAWK1 on the same figure. It should be noted that lanes 1 (pUC19R) and 2 (pCAWK1R) in Figure 1 were loaded with unofficial replicates of pUC19 and pCAWK1only as insurance for running gel electrophoresis and subsequent visualization, and since pBR322 and pCAWK2 were lacking replicates, data from these replicate lanes were excluded during the interpretation of results. Hence, pUC19R and pCAWK1R were only displayed in Figure 2 to emphasize that pUC19 consistently produces the highest IDV, but the data were excluded from further calculations processed in Table 4. Table 5 shows proportional (ratio) comparisons of PCR product amplifications; for example, column 1 features IDV/bp of pCAWK1 divided by the IDV/bp of pBR322. The value 0.90 (below 1) indicates that pBR322 PCR

**TABLE 2** Whole Cell PCR Reaction Components.

| Component | Volume(µl) |
|---|---|
| 10X PCR Buffer (Invitrogen kit) | 2.5 |
| 50mM dNTP's (Invitrogen kit) | 0.2 |
| 0.1M MgCl2 (1.5mM) (Invitrogen kit) | 1 |
| Template DNA (2-20ng) Supernatant from whole cell PCR | 6 |
| Forward Primer (1mg/ml) | 0.1 |
| Reverse primer (1mg/ml) | 0.1 |
| Taq polymerase (5units/ul) (Invitrogen, Cat. #10342-053) | 0.2 |
| Sterile $dH_20$ | 14.6 |
| Final Reaction Volume | 25 |

product is more abundant (ie. higher plasmid copy number).

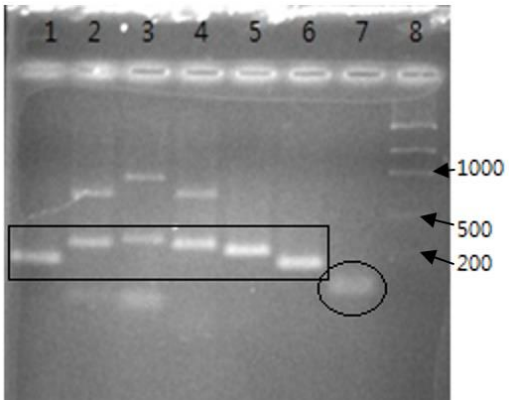


**FIG 1** 1.5% agarose gel. Lanes 1 to 8 were loaded in the following order: pUC19, pCAWK1, pCAWK2, pCAWK1, pBR322, pUC19, negative DNA control (circled), and molecular weight standard 100bp plus GeneRuler by Fermentas. The bands of interest in lanes 1 to 6 are boxed in.

**TABLE 3** AlphaImager analysis of DNA bands on 1.5% agarose gel.

| Lanes | Integrated Density Value ($10^6$) | % |
|---|---|---|
| **1** | 24 | 9.3 |
| **2** | 24 | 9.2 |
| **3** | 24 | 9.2 |
| **4** | 31 | 12.0 |
| **2** | 23 | 8.9 |
| **3** | 17 | 8.5 |
| **4** | 20 | 7.7 |
| **5** | 35 | 13.3 |
| **6** | 39 | 14.9 |
| **7** | 20 | 8.8 |
| **8** | Molecular Weight 100bp plus GeneRuler | N/A |

## DISCUSSION

Ethidium bromide intercalates between base pairs in double helices, leading to brighter bands for larger molecules (13). Therefore, the IDVs were divided by PCR product sizes (base pairs) to calibrate for the differences that size can make on the pixel count measured by the machine. This normalization step is significant since pUC19 produces a smaller PCR product than those of pBR322, pCAWK1, and pCAWK2. According to both visual observation of the gel (Figure 1) and IDV/bp calculations in Table 4, pUC19 PCR product seems to be the more abundant in comparison to pBR322 as theoretically expected, and was also more prominent than either of the pCAWK plasmids. The results may be indicative of many things, including that Rop protein may not have a primary role in the exclusion effect as this study intended to explore. The experiment is much too elementary to be conclusive, however, and would have been informative only had pCAWK bested pUC19 and pBR322 in plasmid copy number, and even then further testing would have been required to be definitive. This is obviously due to the fact that the different combinations of factors potentially involved in causing the exclusion effect are numerous as previous described. Alternatively, this experiment may be indicative of the fact that pCAWK is not an operative *rop* gene mutant. While the *rop* gene was successfully disrupted sequentially via stop codons present in the insert, pCAWK had not been experimentally

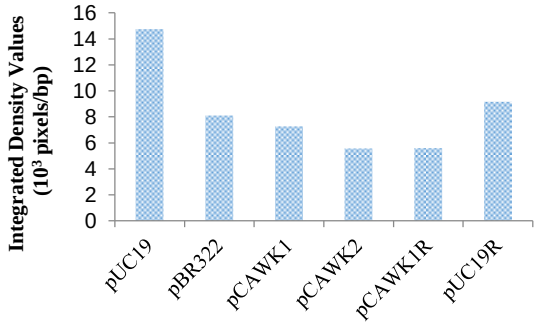


**FIG 2** Normalized Integrated Density Values (IDVs) to show the relative presence of the different plasmids in the cells. Raw IDVs measured y the machine were divided by the corresponding fragment size of the PCR products.

observed to produce a non-functioning Rop protein and was only presumed as such.

Table 4 shows that plasmid copy number is proportionally lower for pCAWK when compared to those of pUC19 and pBR322. Additionally, pCAWK2 copy number was lower than pCAWK1 copy number. This distinction is interesting and can be the result of various causes. Size-wise, both pCAWK plasmids are larger than pUC19 by 1709 bp, and even pBR322, albeit by a negligible amount of 34 bp. It is thus understandable that pUC19 would be able to replicate and accumulate faster in the host than would pCAWK1 or pCAWK2. While the effect of the G to A point mutation in pUC19 and the aforementioned size factor may account for pUC19, pBR322 is sequentially identical beyond the 34 bp insert and should have, had Rop any negative regulatory influence, displayed lower copy numbers than the pCAWK plasmids. Further, pCAWK1 and pCAWK2 are identical save the orientation of the 34 bp insert yet the difference in the amplification of PCR products indicates otherwise. These observations point to a possible flaw in the PCR process, and since the whole cell PCR protocol was derived from previous studies (10), primer design may be the most obvious source of error.

Primer design require adherence to several guidelines. These include considerations for size (optimally, 18 to 22 bp), primer melting temperature (optimally, 52 to 58°C), primer annealing temperature, GC content (optimally, 40-60 %), and possible secondary structures, formed via intra or intermolecular interactions (7). In terms of size, all four primers for pCAWK were of appropriate length, and the GC content as well as melting temperatures fell in the aforementioned optimal ranges (refer to Table 5). Shaded rows display values for the extraneous fragments that were not the PCR products of interest observed in pCAWK lanes as seen in Figure 1, Lanes 2 – 4. Since primer melting temperatures are estimates of the annealing

**TABLE 4** Effect of plasmid type on the subsequent ratio of plasmids in co-infected host cells.

| Plasmid | pBR322 | pUC19 | pCAWK1 |
|---|---|---|---|
| pCAWK1 | 0.90 | 0.81 | -- |
| pCAWK2 | 0.69 | 0.62 | 0.76 |
| pBR322 | -- | 0.89 | -- |

Note: Data calculations exclude the pCAWK1 and pUC19 replicates in lanes 1 and 2.

**TABLE 5** Characteristics of the primers constructed by Integrated DNA Technologies (IDT).

| Plasmid | Tm (°C) | Primer Size | gc% |
|---|---|---|---|
| pCAWK1: | F: 57.4 | 20 | 55 |
| A – B | R: 56.8 | 20 | 50 |
| pCAWK2: | F: 57.3 | 19 | 63 |
| B – A | R: 55.8 | 20 | 55 |
| pBR322 | F: 56.1 | 20 | 55 |
| | R: 55.4 | 20 | 50 |
| pUC19 | F: 54.8 | 20 | 50 |
| | R: 55.3 | 20 | 55 |

temperature, the annealing temperature used to conduct the PCR reactions per plasmid primer set was determined by taking the average of the melting temperatures of forward and reverse primers (7). Because the annealing temperatures of not just pCAWK but also pUC19 and pBR322 primers were either 56 and 57°C, all PCR reactions were concurrently conducted at 56 °C. As for secondary structures, sequences that yielded the fewest palindromes were selected since the presence of these would be conducive to hairpin loops and other intra or intermolecular interactions, which would in turn impede the full potential of PCR amplification. Despite careful design the pCAWK primers lack empirical testing. Contrarily, both pUC19 and pBR322 have long been active tools in molecular biology, with an ample library of primers previously tested by established research. A notable detriment for the pCAWK primers in this paper is that the sequences, especially those of pCAWK2, have higher occurrences of palindromes than pUC19 or pBR322 that could lead to the primers folding in on themselves or forming intermolecular interactions with other primers in solution, reducing the probability of amplifying the region of interest on the plasmid (asterisks in Table 1). This could have hence skewed the results in favour of pUC19 or even pBR322.

Another indication that the primers are flawed is that there are the multiple fragments visible in each of the lanes for pCAWK1 and pCAWK2 (pCAWK1: lanes 2 and 4) and (pCAWK2: lane 3), revealing other regions with priming potential. Primer non-specificity is a disadvantage because, like palindromes, the priming probability of the actual area of interest is dampened. These additional bands may be telling of some other information, however, and are thus worth some scrutiny. Since both pCAWK plasmid PCR products were predicted to mimic that of pBR322 in size (Table 1), the additional and larger fragments in the pCAWK lanes may simply be artifacts. Their lower intensities (lower IDV values as can be found in shaded rows of Table 2) reveal that they are unlikely to be the chief priming sites for the primers. Superficial interpretations may blame the crude nature of whole cell PCR for producing unrefined DNA templates. However, while all plasmids have a common *E. coli* DH5α host and had been processed identically, pUC19 and pBR322 PCR products produced a single band without any extraneous fragments. Hence, this phenomenon must be pCAWK-specific. The pCAWK2 construct was especially problematic since it had the lowest IDV. In the lane for pCAWK2, another faster running band is visible; this is most likely aggregated primers (again, higher chances of inter/intramolecular interaction than the primers for the other plasmids) and dNTP's.

The final and ultimate failing with this experiment is the lack of reproducibility and replicates. Reproducibility is vulnerable to researcher technique as well as the colony selected for the whole cell PCR process since plasmids replicate heterogeneously in individual host cells.

## FUTURE DIRECTIONS

For a more definitive quantification method of plasmid copy number, the real-time qPCR method described in the study by Lee *et al.* can be applied (6). Additional work can be done to perfect the primer sequences for the two pCAWK plasmids to optimize band amplification and explore the extraneous bands that occur beyond the intended region of interest. Further, various annealing temperatures can be attempted; an easy way to determine optimal annealing temperature beyond that found here is to perform a temperature gradient PCR for each plasmid. Pursuing this admittedly time-inefficient approach may reveal inconsistencies in the amplification output caused by varying PCR conditions. This is obviously an issue since if poor PCR conditions abridge proper amplification contrary to the actual quantity of available template in the cell (ie. plasmids), then the output would be less and hence unreflective of the plasmid copy number. In light of this, other ways to optimize the whole cell PCR process overall may abet this endeavor. Previous studies in ameliorating PCR reactions may be valuable reference points (12, 14, 15). Future experiments should also consider using washed broth grown samples to reduce PCR output variability.

## ACKNOWLEDGMENT

This project was supported by the Department of Microbiology and Immunology and Nick Cheng and Lando Robillo, as well as the tireless guidance of Dr. William Ramey. Warmest of thanks to everyone involved and mentioned.

## REFERENCES

1. **Airo A, Changizi F, Kim M, Wibowo J**. 2012. Construction of pCAWK, a novel pBR322-derived plasmid with insertional inactivation of the *rop* gene. J. Exp. Microbiol. Immunol. **16**: 129-135.
2. **Balbas P, Bolivar F**. 2004. Back to basics: pBR322 and protein expression systems in *E. coli* Methods Mol. Bio. **267**: 7-90.
3. **Cell Biosciences**, Inc. 2010. AlphaImager HP, EP, and EC User Guide.

4. **EMBOSS explorer**. "Palindrome." Web 12 Nov. 2012. <http://emboss.bioinformatics.nl/cgi-bin/emboss/palindrome>.
5. **Jew L.** 2011. Troubleshooting the single-step PCR site-directed mutagenesis procedure intended to create a non-functional *rop* gene in the pBR322 plasmid. J. Exp. Microbiol. Immunol. **15:** 142-147.
6. **Lee C, Kim J, Shin S, Hwang S.** 2006. Absolute and Relative quantification of plasmid copy number in *Escherichia coli*. J. Biotechnol. **3**: 273-80.
7. **Premier Biosoft**. "Primer Design." Web 12 Nov. 2012. <http://www.premierbiosoft.com/tech_notes/PCR_Primer_Design.html>.
8. **REPFIND**. Web 13 Nov. 2012. <http://zlab.bu.edu/repfind/form.html>.
9. **Rozen S, Skaletsky H.** Whitehead Institute for Biomedical Research. 2007. "Primer3." Web 25 Oct. 2012. < http://frodo.wi.mit.edu/>.
10. **Tong K.** 2011. Construction of pBAD-clones using the TOPO TA cloning system. J. Exp. Microbiol. Immunol. **15**: 136–141.
11. University of Western Ontario Biology. "Rop Protein." *University of Western Ontario.* PowerPoint. Date. 15 October 2012. <http://*instruct.uwo.ca/biology/3596a/Lecture3.ppt*>.
12. **Venkatram S.** "Analyses of gene disruption by whole-cell PCR using the GoTaq® Green Master Mix." Web 9 Dec. 2012. <http://www.promega.com/ru-ru/resources/articles/pubhub/enotes/analyses-of-gene-disruption-by-whole-cell-pcr-using-the-gotaq-green-master-mix/>.
13. **Waring, M.** 1965. Complex formation between ethidium bromide J. Mol. Biol. **13**: 269-282.
14. **Yang A, Yen C**. PCR Optimization of BOX-A1R PCR for microbial source tracking of *Escherichia coli* in waterways. J. Exp. Microbiol. Immunol. **16**: 85-89.
15. **Zhu J.** 2010. Comparison of four template preparation methods and optimization of BOX A1R PCR for DNA fingerprinting of *Escherichia coli* isolates. J. Exp. Microbiol. Immunol. **14**: 153-160.